

Solid Oxide Fuel Cell Hybrid System for Distributed Power Generation

Semi-Annual Technical Progress Report July 2003 to December 2003

Faress Rahman, Nguyen Minh
January 2004

Performed under DOE/NETL Cooperative Agreement
DE-FC26-01NT40779

Hybrid Power Generation Systems, LLC
19310 Pacific Gateway Drive
Torrance, CA 90502

Disclaimer

“This report was prepared as an account of work sponsored by an agency of the United States Government. Neither the United States Government nor any agency thereof, nor any of their employees, makes any warranty, expressed or implied, or assumes any legal liability or responsibility for the accuracy, completeness, or usefulness of any information, apparatus, product, or process disclosed, or represents that its use would not infringe privately owned rights. Reference herein to any specific commercial product, process, or service by trade name, trademark, manufacturer, or otherwise, does not necessarily constitute or imply its endorsement, recommendation, or favoring by the United States Government or any agency thereof. The views and opinions of authors expressed herein do not necessarily state or reflect those of the United States Government or any agency thereof.”

Abstract

This report summarizes the work performed by Hybrid Power Generation Systems, LLC (HPGS) during the July 2003 to December 2003 reporting period under Cooperative Agreement DE-FC26-01NT40779 for the U. S. Department of Energy, National Energy Technology Laboratory (DOE/NETL) entitled "Solid Oxide Fuel Cell Hybrid System for Distributed Power Generation". The main objective of this project is to develop and demonstrate the feasibility of a highly efficient hybrid system integrating a planar Solid Oxide Fuel Cell (SOFC) and a micro-turbine. In addition, an activity included in this program focuses on the development of an integrated coal gasification fuel cell system concept based on planar SOFC technology. Also, another activity included in this program focuses on the development of SOFC scale up strategies.

Table of Contents

Disclaimer	i
Abstract	ii
Table of Contents	iii
List of Figures.....	iv
List of Tables	iv
Executive Summary	1
Experimental	2
Results and Discussion	2
1 Task 1A.1 – System Design	2
2 Task 1A.2 – Technical Barrier Resolution	21
3 Task 1A.4 – Coal Based System Study	29
4 Task 2.1 – Subscale System Demonstration	29
5 Task 2.3 – SOFC Scale-Up for Hybrid and Fuel Cell Systems	32
Conclusion	33
References	33

List of Figures

Figure 1 Sensitivity of System Efficiency and Power due to Cell voltage and Cell Utilization for Concept 1 (at 80% fuel utilization and 0.75 V).....	3
Figure 2 Sensitivity of System Efficiency and Power due to Cell Voltage and Utilization for Concept 2 (at 80% fuel utilization and 0.75 V).....	4
Figure 3 Sensitivity of System Efficiency and Power due to Cell Voltage and Utilization for Concept 4 (at 80% fuel utilization and 0.75 V).....	4
Figure 5 Schematic of the Integrated COE Model	8
Figure 6 Historical Natural Gas Price	9
Figure 7 Cell Voltage and Fuel Utilization Sensitivity on COE for Concept 1	10
Figure 8 Cell Voltage and Fuel Utilization Sensitivity on COE for Concept 2	10
Figure 9 Cell Voltage and Fuel Utilization Sensitivity on COE for Concept 4	10
Figure 10 System Power as a Function of the Parallon75 Shaft Speed	13
Figure 12 System Efficiency as a Function of Net System Power	14
Figure 15 Rank for Anode Temperature Control Strategies	17
Figure 20 Heat Exchanger Design	22
Figure 21 Pictures of Heat Exchanger Test Setup	23
Figure 22 Heat Exchanger Results	24
Figure 23 Photo of Single Cell Radial Sealless Module Installed in Pressure Vessel	25
Figure 24 Fixed Flow Polarization Curve Taken in Pressure Vessel 1 on Radial Sealless Single Cell Module at Different Pressures	26
Figure 25 Fixed Flow Polarization Curve Taken in Pressure Vessel 2 on a Radial Sealless Single Cell Module at Different Pressures	27
Figure 26 Polarization Curve at 60% Fuel Utilization Taken in Pressure Vessel 2 on a Radial Sealless Single Cell Module at Different Pressures	27
Figure 28 Demonstration Concept Selection Pareto	30
Figure 29 Turbomachinery Selection Pareto	31

List of Tables

Table 2 System Performance Analysis Results Summary	4
Table 3 Systems Performance Analysis Results (at 75% fuel utilization and cell voltage of 0.75V)	4

Table 4 Reliability Results (at cell voltage of 0.75V and fuel utilization of 80%)...	5
Table 5 Availability Results (at cell voltage of 0.75V and fuel utilization of 80%) .	6
Table 6 System Cost Results (at cell voltage of 0.75V and fuel utilization of 80%)	7
Table 7 Summary of COE Results (at cell voltage of 0.75V and fuel utilization of 80%).....	9
Table 8 Summary of System Results	11
Table 9 Design Trade Off Results	11
Table 10 Natural Gas Compressor Operating Points	12
Table 11 Approx Gas Composition Used for Coupon Testing.....	21
Table 12 Sample Heat Exchanger Performance Test Data.....	24
Table 13 Sample Heat Exchanger Performance Results	24
Table 14 Summary of Single Cell Module Pressurized Tests.....	25

Executive Summary

During this reporting period the conceptual design of the full-scale hybrid system, incorporating a Honeywell Parallon 75 microturbine and planar solid oxide fuel cell (SOFC) has been completed. Four system concepts were considered. System concept 4 was downselected. This system concept is estimated to have over 65% efficiency and the highest reliability and availability compared to the other four system concepts evaluated. The down selected system is estimated to have a first cost of \$646/kW and a cost of electricity of 8.4 cents/kW-hour. Part-load analysis of this system showed that the efficiency of the system remains over 60% down to power levels of 200 kW. Several trade studies were completed that are associated with the control of this system. These trades helped develop an understanding of the controllability of the system and investigate strategies for controlling the proposed system.

The high temperature heat exchanger barrier resolution task (1A.2.1) has been completed. Performance tests of the prototype heat exchanger yielded heat transfer and pressure drop characteristics consistent with the heat exchanger specification. Coupon testing on Inconel 625 and Haynes 230 samples completed over 3000 hours of exposure to SOFC conditions. A correlation of the oxide layer thickness as a function of time has been determined from the coupon sample data at three temperatures.

Testing of SOFC cells at pressure continued. Two pressure vessels, both capable of testing multi-cell stacks up to 4 atm, have been set up and validated. Over twenty tests in these vessels have been performed. A performance life test was completed having over 400 hours duration with over 200 hours at 4 atm. Preliminary results from this test indicate higher cell performance degradation at 4 atm. Preparation is underway to repeat this test and validate this conclusion with additional data.

The coal-based integrated gasification fuel cell combined cycle system (IGFC) task has also been completed. The downselected and alternate systems are estimated to have over 53% efficiency. The impact of carbon dioxide removal was estimated and several trade studies on these systems were completed. The final report for this task is currently being prepared and is expected to be submitted by Jan 31, 2004.

Phase 2 of the program has been kicked-off. Several potential system configurations were identified for the sub-scale demonstration system. One system configuration was down selected based on preliminary system performance analysis.

Finally, the SOFC Scale-up task was kicked-off in October. A functional product specification has been drafted and will be reviewed with DOE/NETL in January. A literature search of applicable system configurations has been initiated to support benchmarking and brainstorming of system concepts, anticipated to be completed in the next reporting period.

Experimental

All experimental work currently performed on the program is contained in sub-task 1A.2.1, Barrier Resolution – High Temperature Heat Exchangers and in sub-task 1A.2.2, Barrier Resolution -- Pressurized SOFC. The test procedures and the test methods used to perform the experimental work for these tasks have been described in previous Quarterly Technical Progress Reports.

Results and Discussion

1 TASK 1A.1 – SYSTEM DESIGN

1.1 Conceptual System Design Trade Studies

Previous reports have presented component trade studies conducted to optimize the conceptual design of the full-scale system. Four system concepts are considered.

The down-selection to one system concept is based on system efficiency, reliability, cost, and the cost of electricity (COE). COE provides a means to trade system efficiency against reliability and cost.

The approach undertaken in the trade study consists of the following steps:

- (1) The efficiency of all system concepts is analyzed as functions of system parameters;
- (2) A local maximum of the resulting system efficiency function is determined for each system concept;
- (3) System components are identified for each candidate system concept (some components may be common across the candidate systems);
- (4) System cost and reliability are estimated;
- (5) COE models are created and system COE is estimated;
- (6) The system design point is adjusted if necessary to improve system COE at the acceptable expense of system efficiency;
- (7) Steps (1) through (6) are repeated until an optimized system design is found for each candidate;
- (8) The system with the “best” optimized solution is down selected.

System performance (efficiency), reliability, first cost, and COE analysis are described in the following sections.

1.2 Performance Analysis

A steady state system performance model is the basis for estimating system power and efficiency for a set of component performance assumptions. The components are modeled in a sequential modular fashion using the ASPEN PLUS steady state platform and its thermodynamic database. The model has been optimized for speed, thus enabling efficient system optimization using a large number of model runs.

The system is optimized at the peak power of the Parallon 75 microturbine, corresponding to its peak speed, while the SOFC design and operating points are varied. Thus, the air flow and pressure is fixed, but the SOFC cell operating voltage, fuel utilization, and total electrical power output is varied to maximize system efficiency while maintaining all design constraints of the system.

In general, efficiency increases as the ratio of the power output from the SOFC stack to that of the turbine increases. This is because the fuel cell is more efficient than the turbine. Thus, at this peak condition there is no firing of fresh fuel to increase the turbine inlet temperature. The stack exhaust temperature and the fuel utilization determine the turbine inlet temperature. However, in order to achieve high component reliability, the turbine inlet temperature is restricted. Similarly, temperature limitations are set for the burners, the recuperators, the high temperature air preheaters, and the stack.

The sensitivity of cell voltage (at 80% fuel utilization) and stack fuel utilization (at cell voltage of 0.75V) on systems efficiency and net system power output is shown in Figure 1 for concept 1. The resulting net power output for concept 1 is in the range of 500 to 900 kW depending on the cell voltage and fuel utilization. The net power output increases as the cell voltage or the fuel utilization increases. This is because the efficiency of the stack increases as the cell voltage or the fuel utilization increases, enabling the power output to be increased. The turbine power output also increases due to increased total inlet fuel flow. The system efficiency is in the range of 60 to 65%, and it increases as the cell voltage or fuel utilization increases.

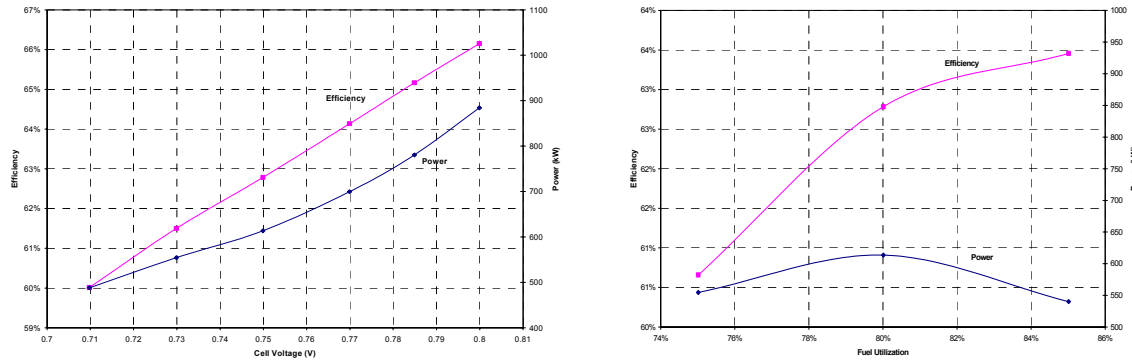


Figure 1 Sensitivity of System Efficiency and Power due to Cell voltage and Cell Utilization for Concept 1 (at 80% fuel utilization and 0.75 V)

The sensitivity of cell voltage and stack fuel utilization on systems efficiency and net power output for concepts 2, and 4 are shown in Figure 2 and Figure 3. A summary of the analysis results for the four concepts is shown in Table 1 and Table 2. The range of cell voltage and fuel utilization considered for each concept remained the same at 0.7 – 0.8 volts and 0.70 – 0.85, respectively.

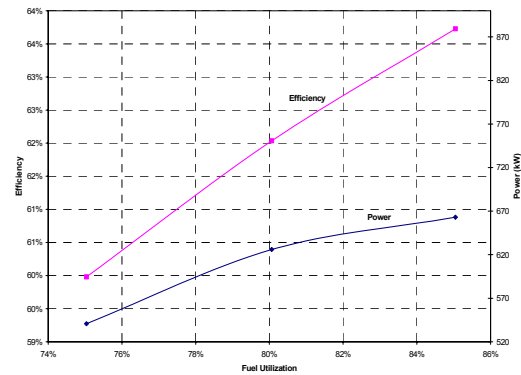
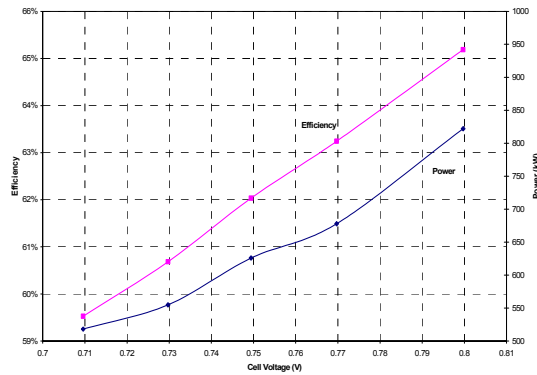


Figure 2 Sensitivity of System Efficiency and Power due to Cell Voltage and Utilization for Concept 2 (at 80% fuel utilization and 0.75 V)

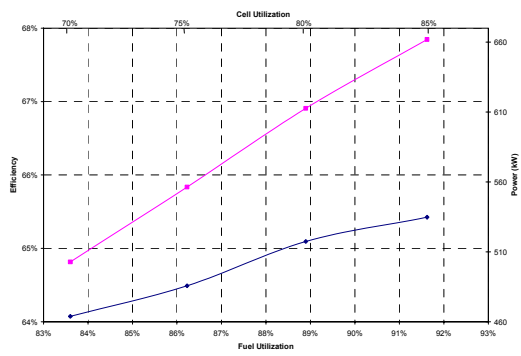
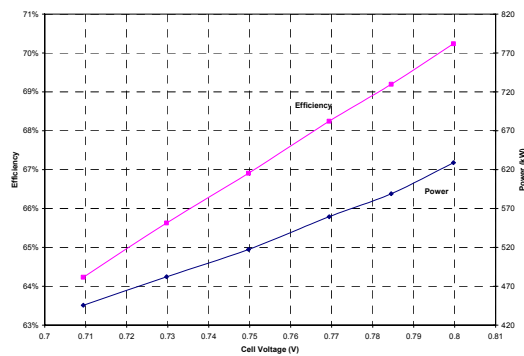


Figure 3 Sensitivity of System Efficiency and Power due to Cell Voltage and Utilization for Concept 4 (at 80% fuel utilization and 0.75 V)

	Concept 1	Concept 2	Concept 3	Concept 4
Net Power, kW	500-900	520-820	200-250	450-650
System Efficiency, %	60-65	60-65	60-65	64-70

Table 1 System Performance Analysis Results Summary

	UOM	Concept 1	Concept 2	Concept 3	Concept 4
Ne Power	kW	614	626	224	517
SOFC Power	kW	563	581	222	495
Turbine Power	kW	86	98	17	78
Efficiency		0.63	0.62	0.64	0.67

Table 2 Systems Performance Analysis Results (at 75% fuel utilization and cell voltage of 0.75V)

The power output from concept 3 is in the range of 200 to 250 kW, less than half of the power achieved by the other concepts. This is mainly due to the low power output from Parallon 75 caused by a low utilization of air. Because of its low power output, this concept is not analyzed as extensively as the others.

The size of the stack depends on the operating voltage and cell utilization in addition to its power level. Operating cell voltage increases as the current density decreases. Similarly, operating fuel utilization can also be increased by decreasing the operating current density while maintaining the same cell voltage. As the current density decreases, the stack size has to be increased to maintain the same power output, thus increasing the total systems cost. Therefore, there is a trade off between the system efficiency and the total systems cost, which directly affects the cost of electricity.

1.2.1 System Reliability Analysis

The reliability of a plant is the probability that the system will perform its intended function without failure under stated conditions for a specified period of time. It can be defined as

$$reliability = 1 - FOF, \quad (1)$$

in which *FOF* is the forced outage factor, the fraction of time the system is forced to shut down and does not include scheduled shutdowns. The system availability is the probability that the system will perform its intended function at anytime, when used under stated operating conditions. Thus it is the fraction of time the system is operational and includes both forced outages and scheduled outages.

Detail life, maximum and minimum repair time, and service interval data was gathered for all major components for each system concept. This data was used to estimate component reliability and availability. These estimates were then rolled up to determine the overall plant reliability for one year of continuous operation and plant availability over 10 years of operation. The number of forced shut downs as well as service maintenance intervals were also estimated to determine operation and maintenance costs. Table 3 and Table 4 summarizes plant level and subsystem level reliability and availability results for each concept. For these calculations the cell voltage and the cell utilization are fixed at 0.75 and 80%, respectively. This assumption is necessary to determine the heat and mass balance through the system and therefore the operating conditions of all the components.

The reliability of Concept 3 is 0.91, the lowest among the four concepts. The reliability of this concept is driven by its need for a high temperature air preheater.

Concept	Total	Subsystems				
		Fuel Processing	Microturbine	Power Electronics	SOFC	BOP
1	0.995	0.998	0.999	0.999999	0.999	0.999
2	0.994	0.998	0.998	0.999999	0.999	0.999
3	0.907	0.999	0.999	0.999999	0.999	0.910
4	0.997	0.999	0.999	0.999999	0.999	0.9998

Table 3 Reliability Results (at cell voltage of 0.75V and fuel utilization of 80%)

Concept	Total	Subsystems				
		Fuel Processing	Microturbine	Power Electronics	SOFC	BOP
1	0.93	0.99	0.98	0.996	0.995	0.97
2	0.94	0.99	0.98	0.996	0.995	0.98
3	0.94	0.99	0.98	0.996	0.995	0.98
4	0.95	0.99	0.97	0.996	0.995	0.996

Table 4 Availability Results (at cell voltage of 0.75V and fuel utilization of 80%)

Component life information was gathered from several sources. The life of the major components of the turbo-machinery was extracted from the detail life analysis reports on the Parallon75 components. The heat exchanger and the other balance of plant data were gathered from publications on previous development programs, including the advanced DOE micro-turbine program and heat exchanger programs. This data has been supported with information gathered from the Internet. The stack and fuel processor life numbers are based on current engineering knowledge and expert opinion.

The basic assumption behind the reliability model is that the components realize wear in time and the probability of failure is not constant over time. Therefore, the Weibull probability of failure is used. The Weibull slope for all components in this study is between 1 and 4, indicative of increasing probabilities of failure as time increases. In such cases, it has been shown in practice that a scheduled replacement may be cost effective. Consequently, in availability calculations when a maintenance interval is identified for a certain component, the component is assumed to be replaced with a new unit and the component life used in the overall plant reliability is assumed to be reset.

A simple rule of thumb was used to estimate the life of high temperature components and also the temperature dependence of their life. The nominal life of these components were assumed to reduce to half their original life for every 25 degree F increase in operating temperature. This rule of thumb assumes no change in materials from the baseline case and is based on expert judgment.

The availability spreadsheet uses a Monte Carlo simulation to estimate the expected plant availability, the standard deviation of the availability calculation, and the expected number of forced and scheduled plant outages. This analysis assumes a normal probability distribution for the life, i.e. a Weibull distribution with beta set at 1.0. This spreadsheet also requires input of the repair time duration for the availability calculation.

1.3 System Cost Analysis

The first cost of the overall system for each system concept was assessed using a cost roll-up model. Component specifications, obtained from system performance analysis, were used to estimate component sizing and then cost. Cost estimates have been made on all major components including the micro-turbine, stack, fuel processor, and the Balance-of-Plant (BOP). The BOP includes the thermal management sub-system, the air, fuel and water delivery sub-systems, and the controls and power electronics subsystems.

All cost estimates have been based on a production volume of 500 units/year or approximately 250 MW per year.

For sub-systems requiring significant technology development, a bottom-up cost model approach was used. For example, a dedicated stack cost model was constructed with the capability to conduct sensitivity analyses. The cost model itemizes the cost into four major components: materials, labor, equipment, and facilities costs. These costs are estimated based on the number of cells and stacks to be build. The total number of

cells and stacks are estimated based on a stack performance model. The model makes a projection of the stack performance in the near future. The fuel processor cost was estimated to be the same as that of the stack. This is consistent with TIAX estimation.¹

Cost estimates for sub-systems containing, to a large degree, currently available technology were derived from quotes obtained from vendors. Adjustments were subsequently made to these quotes to ensure a consistent cost basis. These adjustments were based on engineering judgment. Cost information contained in vendor catalogs were also used as a guide. This approach was used on the micro-turbine, air, fuel and water delivery subsystems and other balance-of-plant (BOP) components. Quotes from vendors, compiled previously for all Parallon 75 micro-turbine, were used as the basis for many of the BOP parts.

Concept No.	1	2	3	4
Systems Cost, \$/kW	545	563	855	646

Table 5 System Cost Results (at cell voltage of 0.75V and fuel utilization of 80%)

Results from the cost model are summarized in Table 5. The cost ranges from \$545/kW to \$855/kW. Concept 3 has the highest cost per kW because its power output is low compared with the other concepts.

1.4 Cost of Electricity Analysis

The Cost of Electricity (COE) model integrates the performance, reliability, and the cost models. A schematic of the information flow is shown in Figure 4. COE is composed of three parts: the cost of fuel, capital cost, and the cost of operation and maintenance.

¹ "Scale-up Study of 5 KW SECA Modules to a 250 kW System", TIAX LLC Final Report to DOE/NETL, Reference: 74313, June 10, 2002

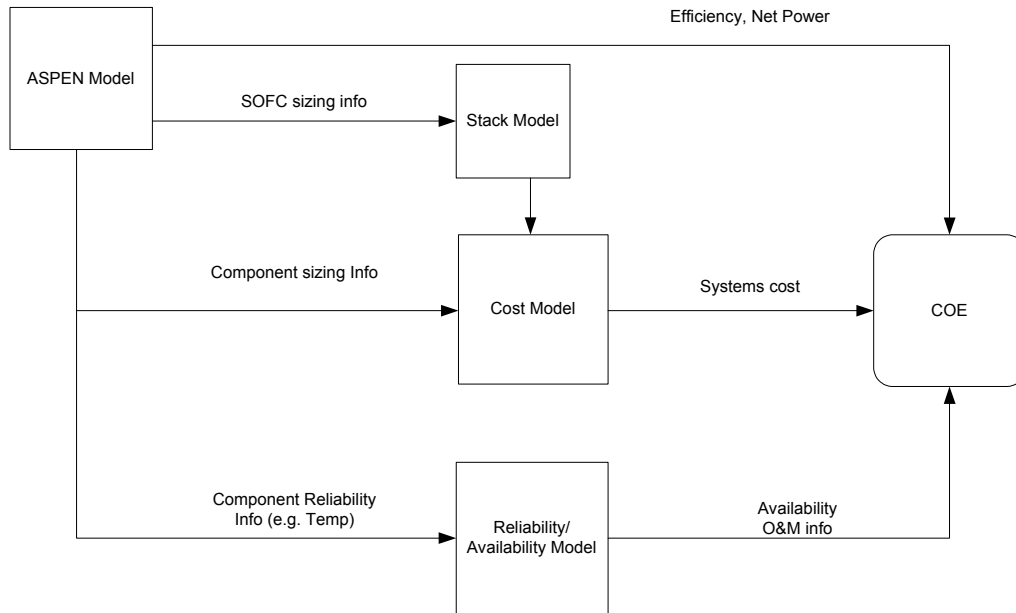


Figure 4 Schematic of the Integrated COE Model

The capitalized cost of the system includes the system manufacturing cost, the installation cost, the other costs associated with installation and operation startup (such as foundation and civil works, and safety systems, etc.) and the owner's costs (owner's engineer, finance costs, etc). The system manufacturing costs, including the microturbine, the stack, the fuel processor, and the Balance-of-Plant (BOP), are estimated in the cost model. The other costs are estimated to be about the same magnitude as the manufacturing costs.

The fuel cost is computed from the total fuel used and the unit cost of fuel. The total fuel used is related to the power plant system efficiency as well as the total power output. The efficiency and net kW output are estimated using ASPEN Plus steady state model. The cost of the natural gas depends on many factors and fluctuates day to day. The historical price of natural gas is shown in Figure 5. The price ranges from \$2 to \$16/MMBtu-HHV. In this analysis it is assumed to be \$6/MMBtu-HHV.

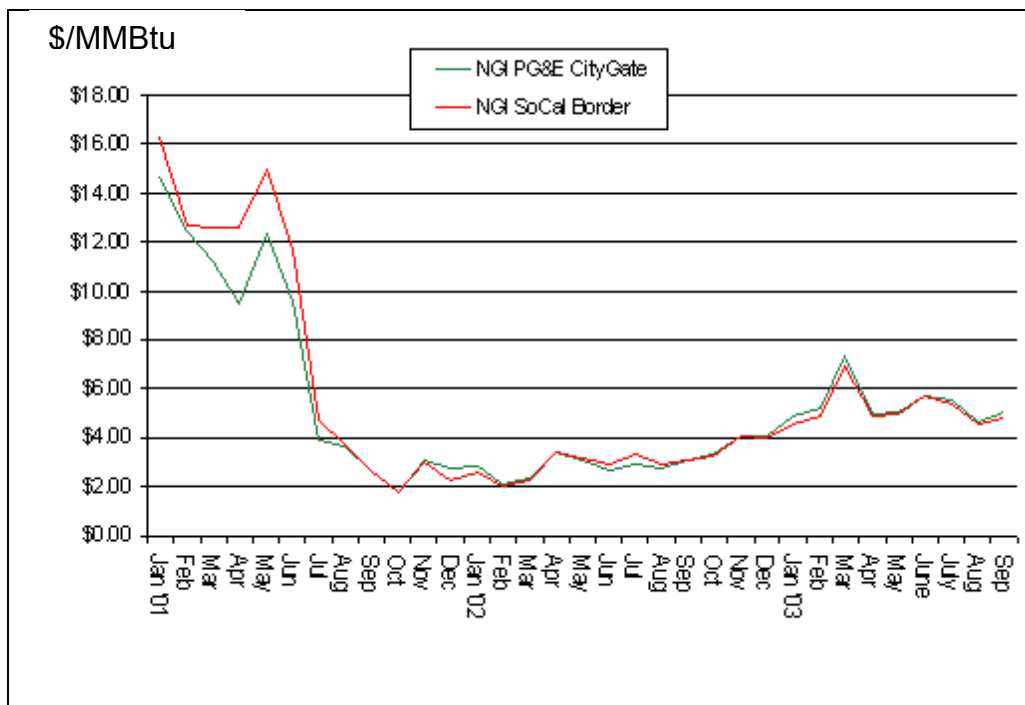


Figure 5 Historical Natural Gas Price²

The operation and maintenance cost are related to the cost and frequency of part replacement and maintenance. The frequency of service is computed using the component availability model described above. The frequency of parts replacement was obtained statistically and the replacement costs were estimated.

Results from the COE model are summarized in Table 6. The cell voltage and the cell utilization are fixed at 0.75, and 80%, respectively for this analysis. The COE of Concept 3 is the highest as a result of its highest capital cost.

Concept No.	1	2	3	4
COE, ¢/kW	8.4	8.1	11.8	8.4

Table 6 Summary of COE Results (at cell voltage of 0.75V and fuel utilization of 80%)

Cell voltage and fuel utilization sensitivity on COE have been evaluated. The results for concept 1, 2 and 3 are summarized in Figure 6, Figure 7, and Figure 8. The cell voltage sensitivity trend on COE is the same as that of cell utilization. At low voltage or utilization the system efficiency is low and the cost of fuel drives the COE high. At high voltage or utilizations the capital cost of the system drives up a high COE. The capital cost is high because more cells has to be added in order to compensate performance

² Source: Bmarkenergy.com

penalty as a result of high fuel utilization. In the case of high cell voltage, more cells have to be added because of decreased power density as a result of increased cell voltage. The minimum COE occurs approximately at a voltage of 0.75 V and a fuel utilization of 0.8 for concept 1 and 2. For concept 4, the minimum occurs at a fuel utilization of 0.75. However, the COE difference at fuel utilization of 0.75 or 0.8 is very small.

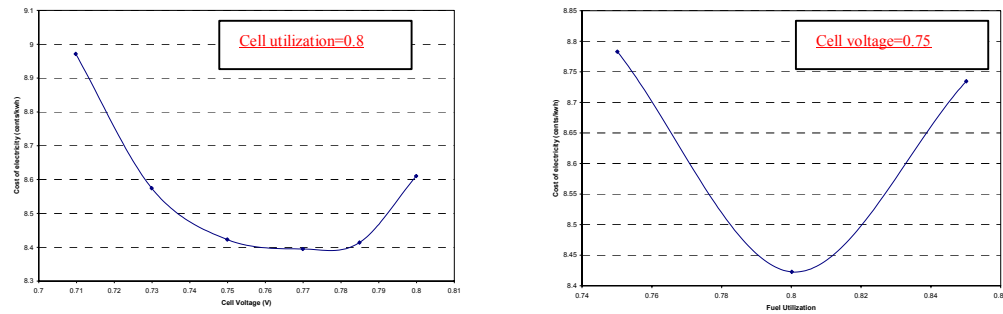


Figure 6 Cell Voltage and Fuel Utilization Sensitivity on COE for Concept 1

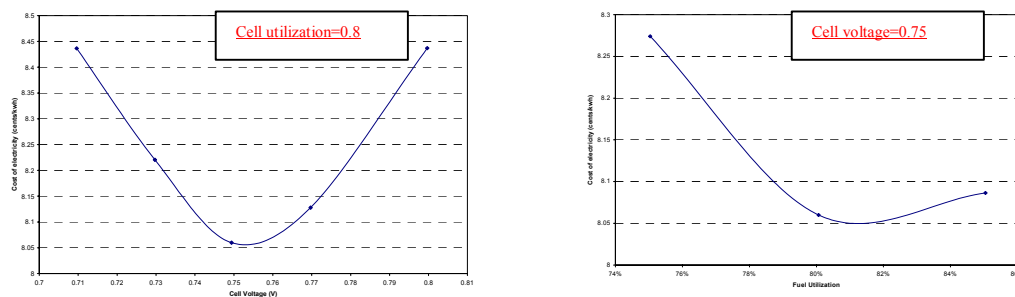


Figure 7 Cell Voltage and Fuel Utilization Sensitivity on COE for Concept 2

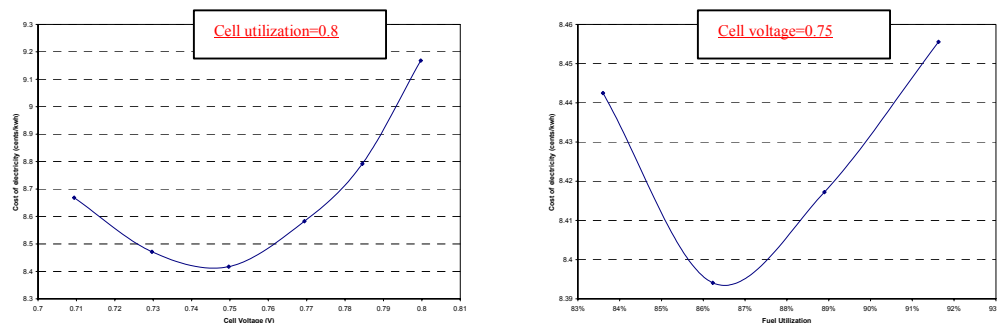


Figure 8 Cell Voltage and Fuel Utilization Sensitivity on COE for Concept 4

1.5 Concept Downselection and Summary

The system concept down-selection is based on system efficiency, reliability, cost, and the cost of electricity (COE). The analysis results are summarized in Table 7. Results are reported with minimum COE. Concept 2 has the lowest COE, but concept 4 has the highest system efficient.

Design for six sigma tools were used trading cost with efficiency. The system variables used to down select a system concept included systems efficiency, availability, and COE. As shown in Table 8, concept 4 received the highest score

	UOM	Concept 1	Concept 2	Concept 3	Concept 4
Net Power	kW	614	626	224	486
SOFC Power	kW	563	581	222	458
Turbine Power	kW	86	98	17	77
Efficiency	%	63%	62%	64%	66%
Reliability		0.995	0.994	0.907	0.997
Availability		0.925	0.940	0.938	0.948
System Cost	\$/kW	545	563	855	634
coe	cents/KWH	8.4	8.1	11.8	8.4

Table 7 Summary of System Results


DOE Hybrid Conceptual Design			System		
 <div> <div>Pass</div> <div>Marg</div> <div>Fail</div> </div> <div> <div>1</div> <div>0.5</div> <div>0</div> </div>					
			Efficiency	Availability	Cost of Electricity
Importance			1	1	1
USL					8
LSL			65	96	
Tolerance			2	2	0.5
Units			%	%	cents/kwh
No.	Concepts	Score			
<input type="checkbox"/> 4	Concept4	0.67	66	94.8	8.4
<input type="checkbox"/> 1	Concept1	0.33	63	92.5	8.4
<input type="checkbox"/> 2	Concept2	0.33	62	94	8.1
<input type="checkbox"/> 3	Concept3	0.17	64	93.8	11.8

Table 8 Design Trade Off Results

1.6 Part-Load performance analysis of the down-selected concept

Following the down selection of the concept system, its performance at partial loads was analyzed. The system performance model was amended for this purpose by inclusion of component performance maps or estimates, particular to the down-selected concept.

The following assumptions were made:

- (1) The Parallon75 recuperator is used. The recuperator performance maps available from Parallon75 test results were included in the model. The recuperator pressure drop curves were also included in the model.
- (2) The fuel cell model was adjusted to reflect the recent changes to the cell baseline.
- (3) The natural gas compressor efficiency was adjusted to lower numbers at partial loads, shown in Table 9. Since no performance maps are available for this component, conservative estimates were adopted.
- (4) The effectiveness of the steam generator, the reformer and the reformat heaters were set to constant values equal to those at the peak power. This is a conservative assumption as the effectiveness of a heat exchanger is likely to improve at lower flow rates due to a longer fluid residence time in the heat exchanger. This assumption is only valid at steady state and for a limited range of power loads because the bypass flows required to control heat exchanger outlet temperatures will likely be significant at unsteady and/or low power conditions. This assumption will be revised and updated during the detailed design phase when heat exchanger maps are available.
- (5) Pressure drops through the system were calculated at partial loads using Aspen's pipe model. The pipe geometry will be adjusted when the piping system design is completed during the detailed phase.
- (6) The SOFC pressure drop was conservatively assumed to be about 4.5% of the inlet pressure.

Fuel Flow, kg/sec	Pressure Ratio	Isentropic Efficiency	Mechanical Efficiency
0.0011	1.45	0.55	0.85
0.0037	1.99	0.60	0.85
0.0097	2.89	0.65	0.85
0.0158	4.19	0.70	0.85

Table 9 Natural Gas Compressor Operating Points

The performance model was used to analyze the system performance at the following Parallon75 shaft speeds: 35 krpm, 45 krpm, 55 krpm, and 64.76 krpm (the design point corresponding to peak power). The system power plot is shown on Figure 9.

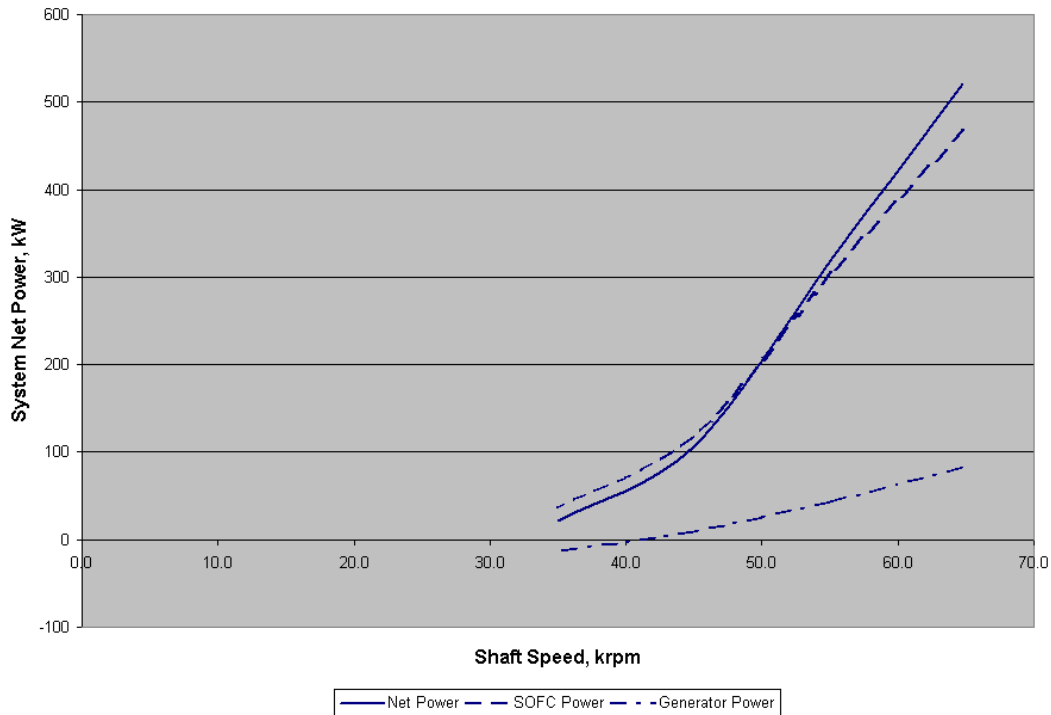


Figure 9 System Power as a Function of the Parallon75 Shaft Speed

Note that the net power is a steep function of the shaft speed. This implies that the system is likely to operate at a speed close to the design speed as long as the power load does not significantly deviates from the peak load.

The microturbine generator power on Figure 9 is negative for shaft speeds below approximately 40 krpm (however, the net system power is still positive). This has implications for the start-up strategy, as the Parallon75 system will have to be operated in the turbocompressor mode rather than the microturbine mode. In other words, the generator would be operated as a motor to drive the compressor. It is recommended to operate the system above 40 krpm at all times in normal operations, if possible to avoid complicated and expensive controls and power electronics solutions.

It should be noted that the control scheme at part loads may have some differences from the peak load control scheme. Particularly, the recuperator inlet temperature requirement was found to have an effect on the average fuel cell temperature at part loads. Since the system operating pressure declines at lower speeds, the turbine pressure ratio is lower as well, which results in higher turbine outlet temperatures. Also, the compressor outlet temperatures are lower because of the lower compressor pressure ratio. This results in a lower fuel cell cathode inlet temperature.

The system efficiency plot is shown on Figure 10. Note that the system efficiency remains relatively flat for the net power higher than about 250 kW (or Parallon75 shaft speed above 50 krpm). The system power in this region is a strong function of two

parameters: (1) the single-cell voltage (the higher the voltage, the higher the system efficiency); and (2) the SOFC specific power, i.e. the ratio of the SOFC power to the cooling air flow rate (the higher the specific power, the higher the efficiency). The voltage rises at lower power loads because the SOFC stack operates at a lower current density. However, this rise is tempered by the decreasing fuel cell temperature and pressure at part load as was discussed above. On the other hand, the specific power tends to decrease with decreasing speed due to the recuperator temperature constraint. The combination of these effects results in a relatively flat efficiency line at higher part loads. However, the SOFC specific power decreases at a faster pace with decreasing system power, which eventually results in lower efficiencies at low part loads.

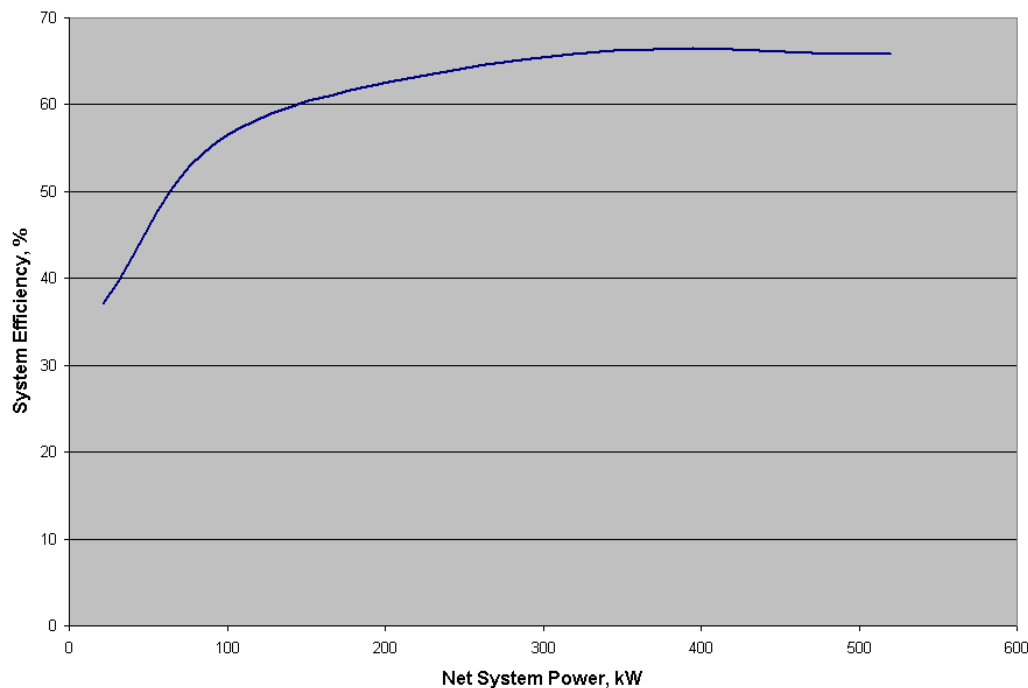


Figure 10 System Efficiency as a Function of Net System Power

1.7 Control System Development

The control system development focused on the following two areas during this reporting period

- Control system trade studies
- Conceptual control system design

The objectives of the control system trade studies are to develop a better understanding of the controllability of the proposed full-scale system and investigate strategies for controlling the proposed system. The control system trade studies identify key controllability issues and are used to develop the conceptual control system design.

The conceptual control system design will be the basis for the preliminary and detailed control system designs during phase 2 and 3 of the program.

For these studies, controllability goals and objectives were established and the impact of the system design on controllability was evaluated. In addition, the trade studies helped prioritize the controllability issues based on system requirements. These trade studies provided feedback to the overall system design so that it can be adjusted to improve its potential operation. Finally, this effort established and validated the basic tools that will be used to design the conceptual and demonstration control systems in subsequent phases of the program.

1.7.1 Control System Trade Studies

Several control system trade studies were brainstormed and prioritized using a Six Sigma tool, the Quality Function Deployment (QFD). This QFD prioritized the trade studies by ranking each with respect to their influences on major system design changes, system cost, system performance, and system reliability, as well as the maturity of the tools needed to execute the trade study. The transient response trade study and bypass temperature control trade studies were significant enough to warrant investigation early in the program. The stack performance sensitivity trade study was not addressed due to the immaturity of the system design and the availability of the part-load model needed for the study. The stack performance sensitivity, stack degradation, startup strategy, and shutdown strategy studies are anticipated to be addressed in subsequent phases of the program during the preliminary and detailed control system designs.

The dynamic system model developed in Matlab/Simulink, discussed in previous reports, was used to conduct the control system trade studies. This model was assembled using GE HPGS' Dynamic Fuel Cell Component Library. The model was verified by comparing its results with the results from the Aspen steady state system performance model of the full system. The full system model or an appropriate subset of the system model was used in each of the control system trade studies discussed below. The combined conceptual control system design was subsequently implemented and validated with the full system model.

1.7.1.1 Bypass Temperature Control

The objective of the bypass temperature control trade study is to determine the location and necessity of bypasses for temperature control during start-up, shutdown, normal operation, and load transitions. During this trade study, the conceptual control system design, proposed earlier in Phase 1 has been revisited to explore different concepts for temperature control. Control strategies were evaluated based on:

- Number of bypass valves
- Location and temperature of bypass valves
- Impact on system capital cost

- Impact on system efficiency
- Controllability/Stability at setpoint
- Response time

The bypass temperature control study will be discussed first in terms of cathode temperature control and then in terms of anode temperature control. These trade studies were performed on the downselected system, system concept 4.

1.7.1.1.1 Cathode Temperature Control

There are two strategies that may provide adequate control of the cathode inlet temperature:

- A. Bypass hot side of recuperator
- B. Bypass cold side of recuperator

Both strategy A and strategy B have the same influence on the cathode inlet temperature. However, since strategy B requires a lower temperature it was selected as a candidate for further investigation.

Simulation studies were conducted using the full dynamic system model to evaluate the performance of the bypass control and tune the cathode inlet temperature controller. While the cathode inlet temperature does not perfectly track the setpoint, the performance of the control strategy is considered acceptable. One risk identified is that the cathode inlet temperature would drop below the lower specification limit if the airflow is greater than 10% of its design point flow rate for more than 30 minutes. However, violation of the lower specification limit may be avoided by decreasing the fuel utilization setpoint (thereby increasing the temperature of air exiting the air preheater) or actively heating the stack. These risk mitigation strategies will be investigated further in subsequent phases of the program.

1.7.1.1.2 Anode Temperature Control

Four strategies were considered to provide adequate control of the anode inlet temperature:

- A. Bypass cold side of fuel preheater
- B. Bypass cold side of fuel processor preheater
- C. Bypass fuel to the fuel processor
- D. Bypass cold side of reformat preheater

These strategies were prioritized using a Six Sigma tool. The strategies were qualitatively evaluated against key elements that are considered critical to quality (CTQ's) for the control strategies. Strategy D is expected to have a strong influence on temperature but requires a high temperature valve. Strategy A does not require a high temperature valve but has a weak influence on anode inlet temperature. Strategy B has a weak influence on anode inlet temperature, but may be important for fuel processor and reformat composition control. Strategy C may have limited utility unless the

stack's internal reforming capability is large and the temperature impact on the stack is explicitly considered in the control algorithms. Strategies A and D were selected as the candidates for further analysis.

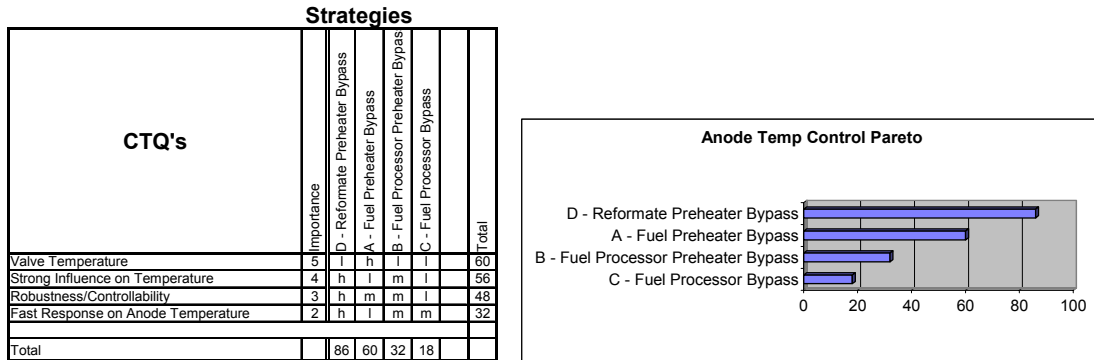


Figure 11 Rank for Anode Temperature Control Strategies

A Matlab/Simulink dynamic subsystem model containing the fuel preheater and bypass, fuel processor, reformate preheater and bypass, and stack is used to analyze the two down selected control strategies. For both strategies, the bypass valve is used to control stack anode inlet temperature with a proportional plus integral (PI) controller.

For Strategy A, the fuel preheater bypass controller is turned on at the full power condition and is not able to maintain an anode inlet temperature with the bypass valve at 100% open. For Strategy D, the reformate preheater bypass controller is turned on at the full power condition and is also not able to maintain an anode inlet temperature, but by a less margin than strategy A. The bypass valve is also 100% open, but direct control of anode inlet temperature provides a more favorable response without the process time delays and thermal lags of the fuel processor that exist with Strategy A. While neither strategy was able to maintain the desired setpoint, strategy A is considered more effective and therefore selected.

Simulation studies were subsequently conducted using the full dynamic system model to evaluate the performance of the reformate preheater bypass control (strategy A) and tune the anode inlet temperature controller.

1.7.1.2 Transient Response

This trade study focused on SOFC/microturbine hybrid system transient behavior. The results from this trade study will be used to develop load sharing control techniques for the microturbine-generator (MTG) and SOFC power systems during load transients and disturbances. A simplified hybrid system model was used to examine the major system components with the goal of qualitatively characterizing gross dynamic interactions. A novel control method has been developed that allows the hybrid system, with power being generated by both the SOFC and MTG, to follow a demanded, transient power setpoint and thus follow load changes in a controllable fashion.

The system concept evaluated in this trade study was based on Concept #1. Major components such as the SOFC, turbomachinery, recuperator, stack heat exchanger, and depleted fuel oxidizer were included in the dynamic system model.

The following recommendations can be made from the results of this trade study.

Minimize Internal Volumes - Internal volumes have a direct impact on controllability, especially during load transitions. The larger the internal volumes of the components and piping of the hybrid system, the more drastic the system responses are to a load change or disturbance. The system can transition faster between load demand setpoints when the volume is minimized. Larger volumes will decrease the transition speed away from the entitlement ramp rate.

Minimize Component Pressure Drops - Each component pressure drop contributes to losses in system efficiency. In addition, larger pressure drops leave less surge margin for the compressor and slow system response—especially during a load decrease. A reliable load transition necessitates adequate margin from surge as disturbances not modeled in this study may require additional margin to keep the compressor from surging.

Incorporate Blow-off Valving - As stated earlier, the volumes associated with the working fluid have a profound effect on the transient performance of the hybrid system. The largest of these will likely be associated with the pressure vessel that will house the SOFC stack. Large volumes slow the system response in that they act as a pressure capacitance, storing working fluid mass. When the system reduces power, the pressure inside the vessel does not decay instantaneously as the MTG speed is reduced. This causes the MTG Compressor performance running line to move towards the surge line. The surging phenomenon is caused by the inability of the compressor discharge fluid momentum to overcome the pressure gradient across the compressor wheel (without momentum, the fluid will tend to flow from high to low pressure, backwards over the compressor wheel—the opposite direction required to operate the hybrid system). In order to reduce the likelihood of surging, the pressure in the SOFC stack containment vessel should be reduced quickly upon MTG deceleration, so that the running line remains away from the surge line. One way to increase the speed in which the pressure vessel volume discharges would be to incorporate a blow-off, or pressure relief valve. This would, if sized correctly keep the compressor away from surge during a load reduction event. The correct placement of the valve, either before or after the stack, should be studied further as a way to increase the transition speed, at least for load reduction.

Incorporate Bypasses - Because of the nature of the single shaft MTG, the turbine expander outlet temperature (TOT) decreases with increasing airflow and system power. This will serve, due to recuperation of the system exhaust heat, to lower the SOFC stack inlet temperature as airflow increases and increase stack inlet temperature as airflow decreases. Thus, there will be one particular airflow and associated enthalpy that will match the SOFC stack for a given current drawn, precluding any variation in stoichiometric ratios. For flexibility in operation (i.e. variation of air stoichiometry),

bypasses around the stack and/or recuperator may need to be incorporated to provide an increased temperature control capability for off-design conditions.

There are some risks associated with the recommendations of the transient trade study. It must be understood that this was a simulation with many simplifying assumptions. The goal, in this case, was to identify trends that should be explored further in the Preliminary and Detailed designs. The quantitative values may not be representative of an actual system, but were used to qualitatively identify hybrid system performance.

One simplification that might have an effect on performance was the transient response of the fuel reformer. This study assumed that the thermodynamics of the fuel reformation process is accounted for, but does not specify the fashion (external, internal, steam, partial oxidation, etc.). A significant limitation might be imposed on the fuel utilization algorithm should the reformer play a critical limitation in transient response.

Another risk was the stack performance model. The current neural network model does not vary performance based on fuel composition—only on overall fuel utilization. It is well known that SOFC performance is dependent on fuel composition as well as fuel utilization. Only hydrogen fuel diluted with nitrogen has been mapped in the current SOFC performance model. Therefore, in addition to the thermodynamic response of the reformer stated above, the fuel composition entering the SOFC stack may impose transient effects not modeled in this study.

The heat loss from the system was assumed to only take place through the SOFC stack pressure vessel wall. Both the value and the location of the actual system heat rejection may have a profound effect on operation and thus might affect the actual transient and steady-state performance of the hybrid system.

1.7.1.3 Control System Trade Study Summary and Conclusions

Several areas were investigated as part of the control system trade studies to identify controllability issues that could influence the conceptual system design and to begin to define how to control the proposed hybrid system. The most important conclusion drawn from these trade studies is that Concept 4 can be controlled.

The transient response trade study looked at the hybrid system and established a preliminary estimated load-change ramp rate of 1500 W/s if the system volumes are minimized. There were many assumptions that went into this estimate and additional analysis with more detailed component information will be needed in subsequent phases of the program to determine the true entitlement of the system. The control strategy developed in the transient response trade study showed that the temperature of the SOFC can be adequately controlled using current draw, with the power demand being met based on feedforward setpoint controls for airflow and some trimming with fuel utilization. This strategy shows great promise in minimizing the temperature fluctuations of the SOFC stack. In subsequent design phases this strategy will be combined with the supervisory controls and the lower level temperature, pressure, and process controls to form the control strategy for the system.

The control system trade studies conducted in Phase 1 of this program were based on preliminary information for component performance and operating constraints. The control system design will need to be updated and optimized as the system definition proceeds, various component designs mature, and more realistic component performance data is obtained.

1.7.2 Conceptual Control System Design

The conceptual control system design for the full-scale system was updated during this reporting period with the results of the control system trade studies. The control structure underwent few changes from that reported in previous reporting periods.

The control structure is divided into two subgroups, the supervisory controls and the active controls. The supervisory controls perform the following functions:

- Translates load demand, user commands, and system status into setpoints for active controls
- Manage operating modes
 - Startup
 - Normal Operation
 - Shutdown
 - Emergency Stop
- Manages Built-In Test (BIT) and alarms

The active controls perform the following functions:

- Feedforward control for fast transitions between setpoints
- Feedback control for disturbance rejection and improved setpoint tracking

The feedforward control takes advantage of a priori information on the system operation to improve the transient response and stability of the system. An example of this would be the setting for the cathode temperature control valve being scheduled as a function of fuel cell power. Therefore when the fuel cell power is commanded by the controller, the appropriate valve position is also commanded. The feedback action of the control system would then fine-tune the position of the valve to achieve the exact cathode inlet temperature setpoint. The feedback portion of the control therefore provides disturbance rejection and robustness to variation in the process or components.

Due to the complexity of the system and its numerous constraints, the supervisory controls must be coordinated with the lower level control loops must also watch all component and system constraints while maintaining the demanded load.

The conceptual control system design has been implemented, tuned, and verified in the full dynamic system model. The supervisory controls have only been implemented to the point of coordinating lower level control loops. The built-in test and health monitoring functions will be added in subsequent phases of the program. The

simulation results show the temperature and pressure constraints around the system are satisfied during rapid load changes of 500 W/s. The fuel utilization is not well controlled with load changes causing large deviations from the targeted value of 80%. This will need further investigation in subsequent phases of the program, but is probably due to the fuel flow control and pressure dynamics associated with the long path fuel must travel before reaching the stack. These oscillations can be limited or removed if the load change ramp rate were further limited.

2 TASK 1A.2 – TECHNICAL BARRIER RESOLUTION

2.1 Subtask 1A.2.1 – High Temperature Heat Exchangers

The objective of this task is to develop, design, fabricate, and test a high temperature heat exchanger capable of operating with high-temperature exhaust gases to heat up air before it is introduced into the fuel cell stack. Prior reports have outlined the design and construction of a demonstration heat exchanger for testing and the analysis of a high temperature heat exchanger for pressure containment and creep life. The pressure containment and creep life analysis is supported with oxidation tests on coupons of representative high temperature materials presented below. Further, the performance testing of a prototypical high temperature is also presented below.

2.1.1 Oxidation Tests

Sixty coupon samples were prepared and placed in three furnaces at different temperatures: 732 °C (1350°F), 800 °C (1475°F), and 900 °C (1650°F). The tested coupons are made out of Inconel 625 and Haynes 230 rods. These samples were exposed to the SOFC combustion environment having gas compositions as described in Table 10. Samples have been scheduled for removal from the furnace at different exposure times ranging from 250 to 5000 hours. Micrographs showing the oxidation of these samples at exposure times up to 315 hour at the three temperatures were shown in previous reports.

Gas	Approx Partial Pressure at 800 °C (1475 °F)
N ₂	0.7922
O ₂	0.1039
CO ₂	0.0346
H ₂ O	0.0693
H ₂	9.73E-11

Table 10 Approx Gas Composition Used for Coupon Testing

The oxide penetration was measured on samples removed from the furnace and correlated with exposure time. The depth of metal attack used in these plots includes the thickness of the oxide layer and the thickness of the depleted zone from which

alloying elements are lost. It should be noted that general literature on oxidation usually is based on the oxide layer alone.

Assuming a required design life of 5000 hours for a high temperature heat exchanger constructed using 0.003-inch thick metal sheets, the data suggests both Inconel 625 and Haynes 230 are suitable for applications up to 730 °C (1350 °F). However, at 800 °C (1475 °F) the Inconel 625 will achieve the design life but Haynes 230 will not.

It should be noted the plots shown in **Error! Reference source not found.** through **Error! Reference source not found.** have been fitted with relatively short exposure data, approximately 3000 hours. Consequently, caution must be exercised in extrapolating this data to longer durations. The conclusions drawn from this data will be reviewed as longer exposure data is obtained.

2.1.2 Heat Exchanger Tests

A series of performance tests were conducted with the prototypical heat exchanger. The heat exchanger design is shown in Figure 12.

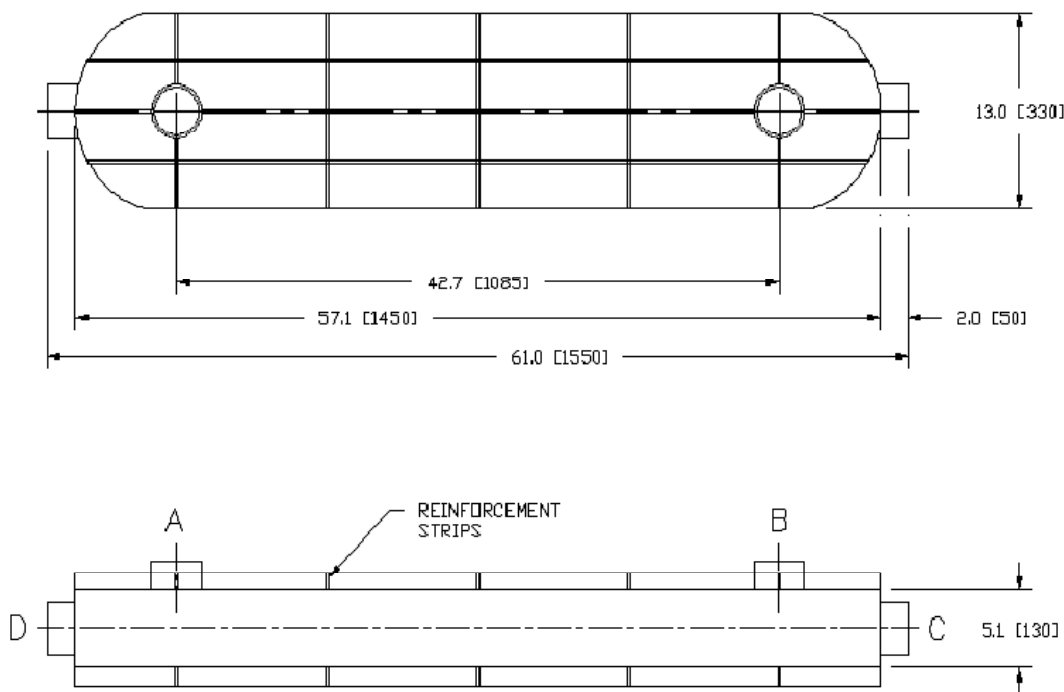


Figure 12 Heat Exchanger Design

The heat exchanger test set up is shown in Figure 13. The tests were conducted according to the following process. Flow rates, temperatures, and pressures were measured at the inlet and exit streams of the heat exchanger. At each operation set point the unit was allowed for the unit to achieve steady state conditions. Temperature and pressure measurements were taken at at-least three points within the duct cross-section to ensure bulk average temperatures were being recorded. At the outlet of the

heat exchanger a mixer was used to measure the mixed flow temperature. The pressure measurement was measured before the mixer, at the outlet of the heat exchanger. All the data was recorded using Lab View data acquisition system. During the test, no anomalies occurred.



Front view



Left side view



Right side view



Thermocouples in heat exchanger skin

Figure 13 Pictures of Heat Exchanger Test Setup

Table 11 and Table 12 show the sample data taken during the performance test and the results computed from the raw data.

Hot Flow Rate (kg/s)	Cold Flow Rate (kg/s)	Hot Inlet Temp (deg K)	Cold Inlet Temp (deg K)	Hot Outlet Temp (deg K)	Cold Outlet Temp (deg K)	Pressure Drop Hot side (psig)	Pressure Drop Cold side (psig)
0.062	0.061	755.224	299.417	389.619	607.909	1.0	0.4
0.068	0.061	755.716	299.470	389.857	611.529	1.3	0.39
0.077	0.061	755.726	299.435	399.017	617.246	1.6	0.39

0.084	0.061	755.022	299.487	416.106	624.106	1.8	0.4
-------	-------	---------	---------	---------	---------	-----	-----

Table 11 Sample Heat Exchanger Performance Test Data

Hot Stream Mean Temp (deg K)	Cold Stream Mean Temp (deg K)	Qmax (W)	Effectiveness	U
572	454	28304	0.68	20.26
573	456	28220	0.68	20.41
577	458	28332	0.69	20.01
586	462	28308	0.71	19.08

Table 12 Sample Heat Exchanger Performance Results

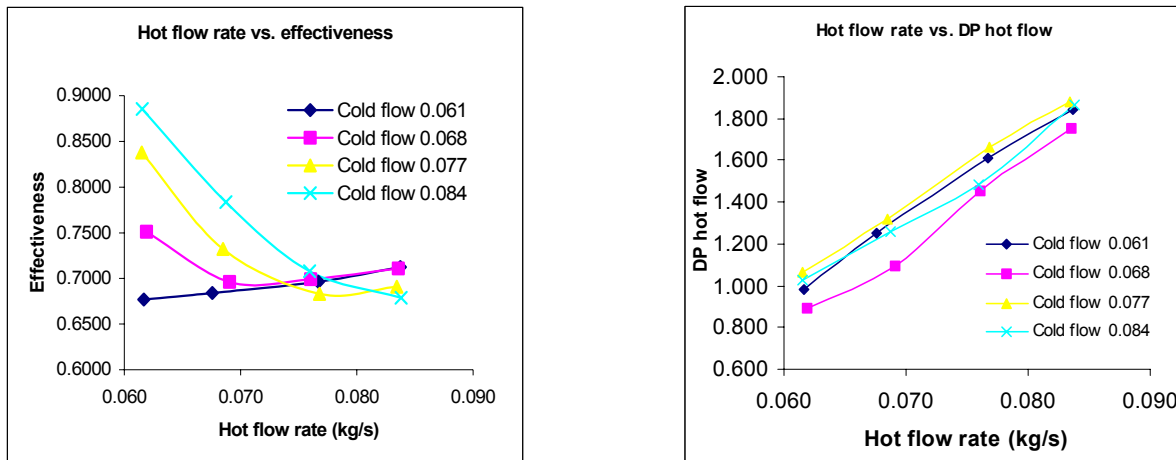


Figure 14 Heat Exchanger Results

Figure 14 summarizes the performance results of the heat exchanger. The heat transfer and pressure drop of the heat exchanger are in good agreement with the design specification of the heat exchanger.

2.2 Subtask 1.A.2. 2 – Pressurized SOFC

Single cell pressurized testing has been performed using two identical pressure vessels that have a stamped vessel rating for 60 psig. Both pressure vessels now reside at GE Global Research Center (GRC) due to construction delays at HPGS in Torrance. Recent efforts have been dedicated to receiving, installing and performing shakedown tests on the second pressure vessel at GRC.

2.2.1 Single Cell Pressurized Testing

A number of single cell pressurized tests have been performed to date and a summary of these tests is presented in Table 13. A 4-inch radial sealless SOFC module test

vehicle has been used for all the testing to date. A photo of a single cell test is presented in Figure 15.

Test Stand	Number of Tests Performed	Fuel Composition	Temperature (deg C)	Pressure (atm)
PV # 1	19	64% H ₂ & 36% N ₂	800	1, 2, 3, 4
PV # 2	5	64% H ₂ & 36% N ₂	800	1, 2, 3, 4

Table 13 Summary of Single Cell Module Pressurized Tests



Figure 15 Photo of Single Cell Radial Sealless Module Installed in Pressure Vessel

Representative data from pressure vessel 1 is presented in Figure 16. Constant flow polarization curves at 1, 2, 3 and 4 atm were taken with a dilute hydrogen fuel composition of 64% hydrogen and the balance nitrogen. The performance increased with pressure as expected with the most significant increase occurring between 1 atm and 2 atm.

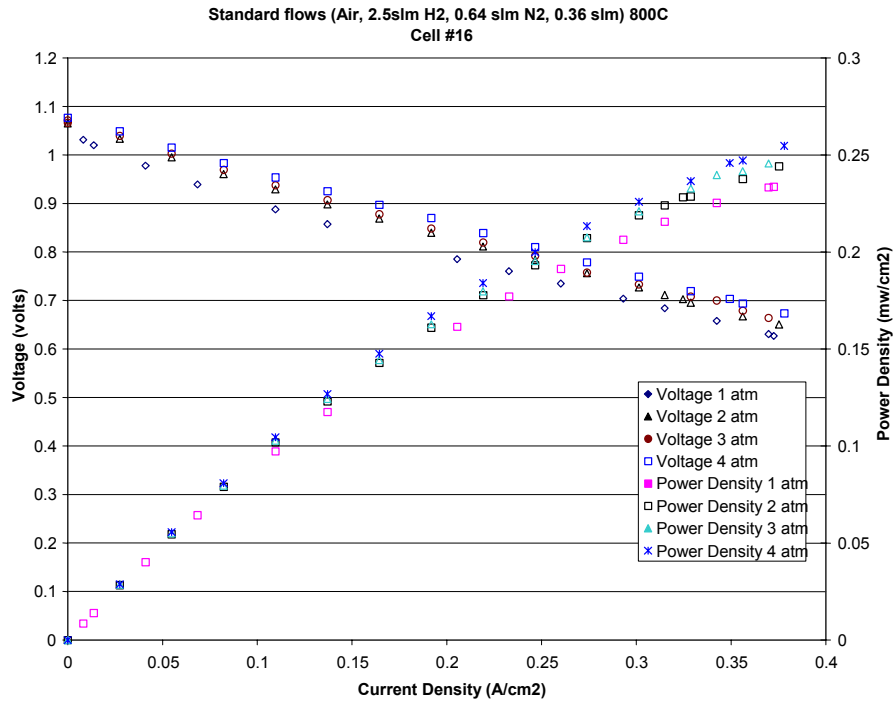


Figure 16 Fixed Flow Polarization Curve Taken in Pressure Vessel 1 on Radial Sealless Single Cell Module at Different Pressures

Data from a radial sealless module using cell #7 tested in pressure vessel #2 is presented in Figure 17. A fixed flow polarization curve was taken at 1, 2, 3 and 4 atm and showed similar performance to the cell tested in pressure vessel #1.

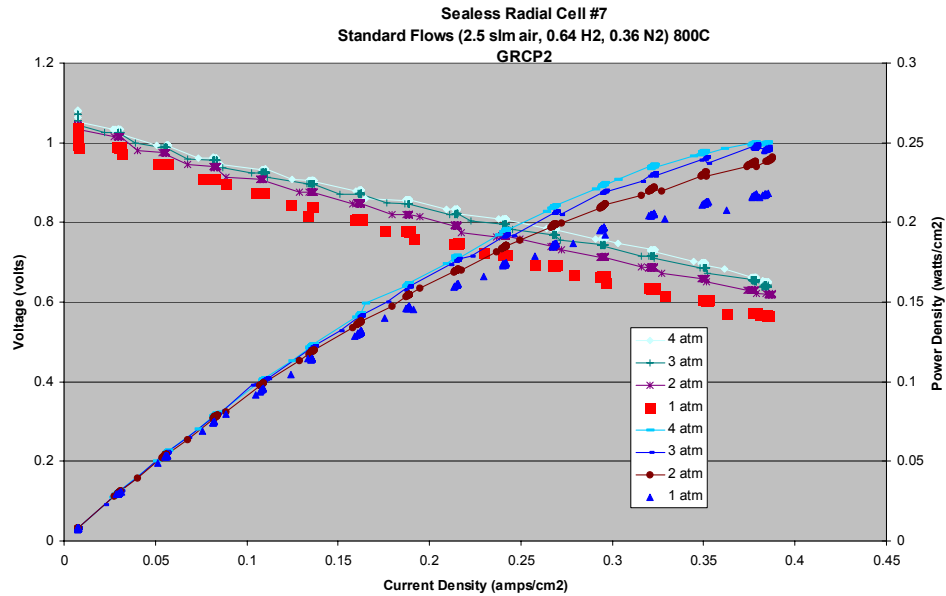


Figure 17 Fixed Flow Polarization Curve Taken in Pressure Vessel 2 on a Radial Sealless Single Cell Module at Different Pressures

Fuel utilization data of 60% was collected for cell number 7 at different pressures and is presented in Figure 18. A few points were also taken at 80% fuel utilization (not shown). The overall power density was lower at the constant fuel utilization points than at the fixed flows.

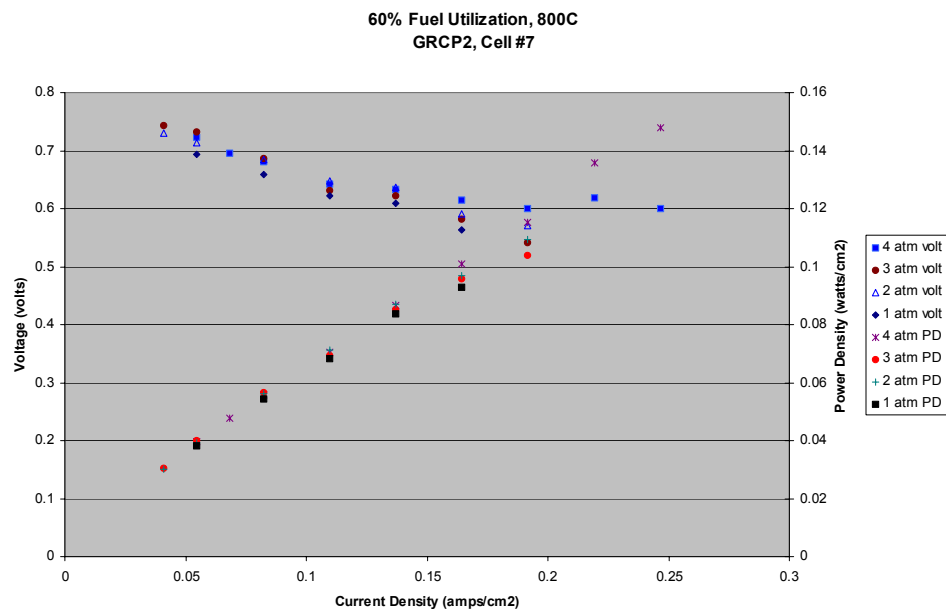


Figure 18 Polarization Curve at 60% Fuel Utilization Taken in Pressure Vessel 2 on a Radial Sealless Single Cell Module at Different Pressures

2.2.2 Carbon Deposition Experiments

In an effort to understand potential degradation mechanisms associated with pressurized operation two areas of study have been initiated: carbon deposition experiments with steam reformed fuel and life testing. Carbon deposition conditions that reduce the cell performance are being evaluated for both ambient and elevated pressure. Life tests are being performed to determine the effect of 4 atm on steady state performance degradation compared to that at 1 atm.

The use of nickel as both the electrochemically-active anode as well as the primary cell support structure (anode-supported cells), while attractive from the perspective of material costs, suffers from a general intolerance to the formation of carbon when utilizing hydrocarbon-based fuels. The problem of carbon deposition is present irrespective of the method of primary fuel reformation such as steam, autothermal, or partial oxidation reformation, and it becomes particularly acute when attempting to incorporate internal steam reformation into system operation. Carbon formation leads to reduced cell performance and it is generally accepted that overall cell failure is greatly accelerated once carbon deposition has begun. From the perspective of system efficiency, carbon deposition occurs at the expense of the overall energy content in the fuel and thus represents a direct loss of cell and system performance.

Thermodynamic calculations can be used to predict the operational space where carbon formation is likely to occur and thus can be used in principle to guide the selection of system operational parameters. However, kinetic studies have demonstrated that factors such as the degree of gas mixing, the local temperature environment, the local composition and nature of the electrode material are important in determining the “practical” carbon deposition rate. Moreover, the gradual change of reformate gas composition and resultant temperature changes occurring along the flow channel due to current generation make the prediction of carbon deposition in a working fuel cell highly complicated. As a result, it becomes important to determine and verify experimentally those operational regions where fuel cell operation can be achieved safely without fear of undesirable carbon formation.

A test approach has been developed to evaluate the cell operating conditions that lead to carbon formation and those that do not. Tests are underway to validate this novel approach.

2.2.3 Life Test

The first life test was completed where a radial sealless cell was tested at ambient and elevated pressure to get a better understanding of the degradation mechanisms associated with testing at higher pressures. The single cell was tested for 224 hours at 1 atm followed by 196 hours at 4 atm at the following conditions: 60% fuel utilization, 20% air utilization, and a current density of 0.16 A/cm². Based on preliminary analysis, the degradation rate was higher at elevated pressure. Test data is shown in **Error! Reference source not found.**

3 TASK 1A.4 – COAL BASED SYSTEM STUDY

The objective of the coal based system study task is to identify and assess highly efficient coal power plant system configurations integrating a coal gasifier and gas cleanup train with a planar SOFC and bottoming cycle. Additionally, this task will identify technology development necessary to realize such systems.

In the current reporting period, analysis of the baseline system configurations were completed and two system configurations were downselected based on system performance, cost, and reliability predictions. The Downselection of these systems were presented to DOE/NETL on September 26, 2003. Subsequently, detailed analysis on these systems, including sensitivity analysis was completed. Further, the feasibility and impact of carbon dioxide isolation was assessed and technology gaps were identified. The results of this analysis were presented to DOE/NETL on January 14, 2004. Currently, a detailed final report is being prepared for submission to DOE/NETL by January 31, 2004.

The proposed plant concepts includes an oxygen-blown gasifier system, a set of fuel cell modules, each containing several stacks, one or two large sized gas turbines, a Heat Recovery Steam Generator (HRSG), and a steam turbine. The possibility of carbon dioxide isolation from the exhaust products, either by an absorption method using Selexol or by pure oxygen combustion, has also been investigated. A rough order of magnitude (ROM) initial capital cost and net plant efficiencies are the top two deliverables for this project.

Given the inherently high efficiency of the SOFC modules, it is necessary to have the entire topping cycle consist of fuel cells. The spent fuel is then burned and the products expanded through large, high efficiency gas turbines. The gas turbine exhaust is then passed through the HRSG and a relatively small steam turbine for additional energy recovery. The carbon dioxide separation unit involves an additional HRSG with the spent fuel on the hot side and steam on the cold side. Most of the fuel cell exhaust is recycled and mixed with the shifted syngas before it is cooled and passed through the Selexol system for carbon dioxide absorption.

Various staging configurations were studied from a thermal management point-of-view. It was decided that the maximum efficiency could be obtained from a staged, intercooled system of SOFC stacks. Various intercooling methods and associated cycle concepts were investigated. A baseline concept (with air recycle) and an alternate concept (with air heat exchange) were downselected for further analysis. Within the error margin of the analysis, both system concepts are expected to have the same cycle efficiency and initial cost. The plant efficiencies ROM costs of these two concepts are expected to be 50-54% and \$1900/kW-\$2100/kW.

4 TASK 2.1 – SUBSCALE SYSTEM DEMONSTRATION

The system definition of the subscale feasibility demonstration system has been defined. The system is at a smaller 5 to 50 kW level. The exact power level of the system will be chosen such that a small commercial turbomachinery can be integrated into the system with minimal development costs while still demonstrating the SOFC stack integration.

4.1 Demonstration System Downselection

Two levels of down selections were conducted. The first level is focused on the system configuration. A brainstorm session was held and over forty ideas were generated. These ideas were then screened and combined into six system concepts.

The down selection criteria for the concepts were established. The main objective of the demonstration is to demonstrate pressure operation of the SOFC stack integrated with a turbomachinery. Thus, emphasize is placed on making a successful integration within the program resource limitations. Based on these criteria, a QFD (quality function deployment) is performed. Concept 5 received the highest score and thus is chosen as the baseline concept. The next highest score is Concept 6. The difference between concept 5 and 6 is the selection of turbomachinery. Thus, further study is performed on the selection of a turbomachinery.

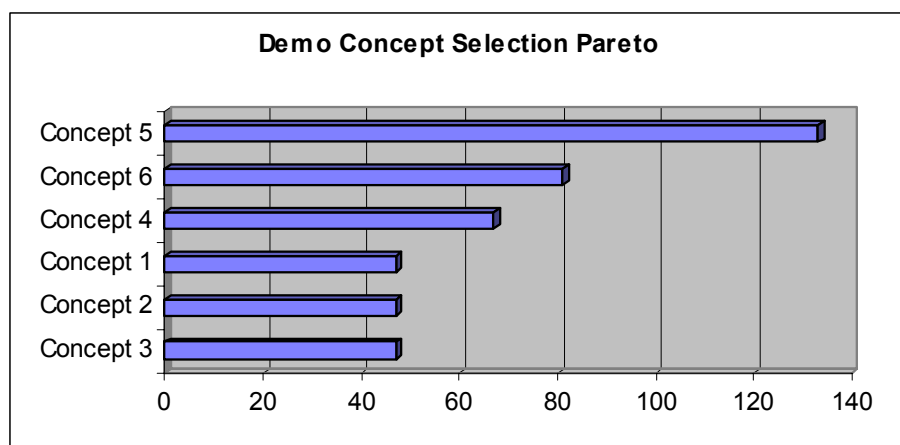


Figure 19 Demonstration Concept Selection Pareto

4.2 Turbomachinery Downselection

A turbomachinery has to deliver pressurized air to the SOFC stack and also recover heat from the stack exhaust. The pressurization part can be achieved by an independent compressor, a compressor as part of a turbocharger, or a compressor as part of a turbogenerator. The heat recovery part can be achieved by an independent turbine, a turbine as part of a turbocharger, or a turbine as part of a turbogenerator. As a result, five combinations were analyzed and a QFD was performed using the same selection criteria as that shown in Table 1. The QFD result is shown in Figure 20. The turbocharger scored the highest mainly because it is available and the performance characteristics are known. Dynajet is a 2.6 kW micro gas turbine generator commercially available in Japan offered by IHI AeroSpace. However, the difficulty associated with integrating this commercial unit with a SOFC stack is not clear. The other concepts involve the development of new components. A summary of the pros and cons of each concept is shown in Table 14.

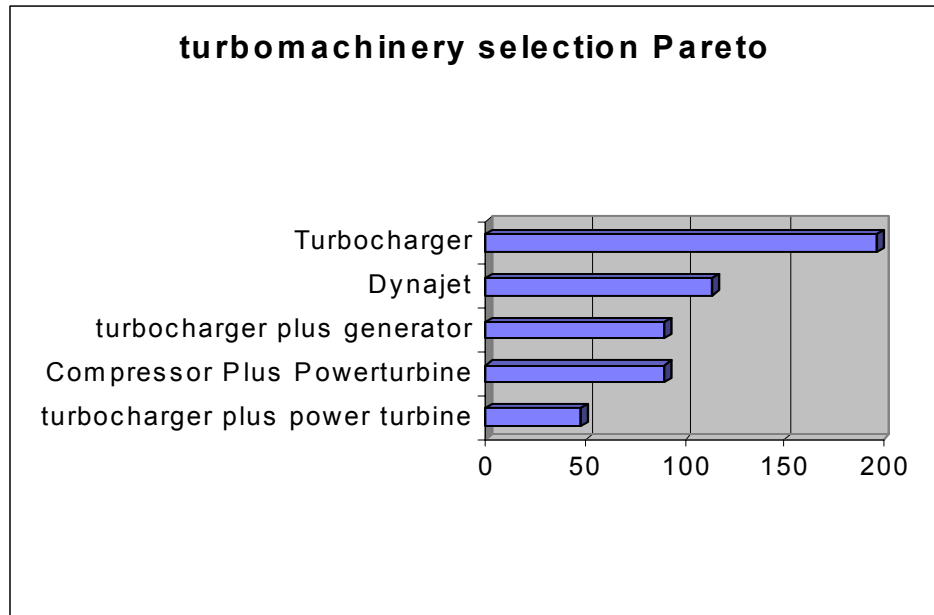


Figure 20 Turbomachinery Selection Pareto

4.3 Demonstration System Control Design

The demonstration system control development was kicked off during this reporting period. A dynamic system modeling strategy was determined and the dynamic demonstration system model was assembled from GE HPGS's Dynamic Fuel Cell Component Library. The dynamic demonstration system model was updated with appropriate performance maps and assumptions. The model's performance was tuned to agree with the steady state system model.

Open loop simulations were conducted to look at model stability and gross dynamics of the demo system. The coupling of the turbocharger with the fuel cell has already presented challenges and it was necessary to manually control the speed of the turbocharger to maintain the proper airflow for the SOFC stack. The dynamic system model is executing stably with an execution speed of 0.2 to 0.5 real-time. The dynamic system model is now mature enough for inclusion of controllers to maintain the desired setpoints for the system. This work will be conducted in Q1 of 2004.

In addition to the dynamic model development, initial assessments were conducted on the six concepts for the demonstration system proposed by the systems team. The six proposed concepts for the demonstration system were qualitatively evaluated for controllability and operability. This input was used with the greater systems team to prioritize the demonstration system concepts for further study. The leading concepts will be quantitatively evaluated for controllability and operability using the dynamic demonstration system model. The concepts that included a generator with the turbomachinery were favored by the controls team, because they supply another degree of freedom for controlling the airflow to the cathode of the fuel cell.

5 TASK 2.3 – SOFC SCALE-UP FOR HYBRID AND FUEL CELL SYSTEMS

GE HPGS has identified a product specification of an SOFC-gas turbine hybrid 20 MW central power generation system (referred to later in the document as the SOFC hybrid product). The product will compete in the centralized generation market space that includes:

- Combined cycle power plants on natural gas
- Nuclear plants
- Hydro power plants
- Old coal (steam) plants
- Large wind farms
- Photovoltaic systems (projected to be available)

GE's FB-class gas turbines or similar systems can be currently considered the closest direct competitors to the proposed SOFC hybrid product. Although FB's size (275MW) is much larger than that of the SOFC hybrid system (20MW+), FB's product requirements will likely be applicable to the SOFC as well. FB's size is driven mostly by gas turbines' property of increasing efficiency with size. On the other hand, the SOFC product will likely have a high efficiency even at 20 MW. However, the SOFC product will have to meet FB's characteristics in order to successfully compete in the central generation market.

GE HPGS has determined that the SOFC hybrid product's competitive advantage over gas turbines will likely be in its lower emissions and higher efficiency relative to competing products. The SOFC hybrid product is not expected to successfully compete in capital cost and reliability, at least initially. However, the SOFC hybrid product will have to meet the competing products' standard for the cost of generated electricity (COE) in order to achieve a significant market share in the future. Therefore, the SOFC hybrid product specification is based on FB-class system specifications and additional SOFC-specific requirements based on internal GE work. The product specification is provided in **Error! Reference source not found..**

The system design will be based on modified GE's internal MW-class SOFC hybrid system design. The baseline design will be modified as necessary to achieve the 20 MW size target. Additional system concepts will be proposed and compared to the baseline. Thermodynamic analyses to determine the concepts' efficiencies will be conducted in the near future.

Available system analysis tools have been identified. Aspen Plus by Aspen Technology, Inc. was selected as the most appropriate thermodynamic analysis tool. Subsystem and component models have been previously developed at GE and will be used in the upcoming thermodynamic studies. Preliminary system models based on the subsystem and component models have been created and are currently under investigation.

Conclusion

The following activities have been carried out during this reporting period. The results from these activities are summarized in this report.

- Optimization of the steady state system performance model
- Construction of the system cost and reliability rollup models
- Control system analysis and trade studies
- Dynamic system model verification
- Testing of high temperature heat exchanger material coupons
- Setup of pressurized SOFC testing facilities, including two pressurized vessels
- Integrated coal gasification and SOFC analysis.

References

“Scale-up Study of 5 KW SECA Modules to a 250 kW System”, TIAX LLC Final Report to DOE/NETL, Reference: 74313, June 10, 2002.